LIMNOLOGY
AND
OCEANOGRAPHY

January 2003
Volume 48
Number 1

Limnol. Oceanogr., 48(1), 2003, 1–8

Extreme water velocities: Topographical amplification of wave-induced flow in the surf zone of rocky shores

M. W. Denny,[1] *L. P. Miller, M. D. Stokes,*[2] *L. J. H. Hunt, and B. S. T. Helmuth*[3]
Hopkins Marine Station of Stanford University, Pacific Grove, California 93950

Abstract

Water velocities as high as 25 m s^{-1} have been recorded in the surf zone of wave-swept rocky shores—velocities more than twice the phase speed of the breaking waves with which they are associated. How can water travel twice as fast as the waveform that initially induces its velocity? We explore the possibility that the interaction of a wave with the local topography of the shore can greatly amplify the water velocities imposed on intertidal plants and animals. Experiments in a laboratory wave tank show that interactions between bores refracted by a prowlike beach can produce jets in which the velocity is nearly twice the bore's phase speed. This velocity can be further amplified by a factor of 1.3–1.6 if the jet strikes a vertical wall. This type of topographically induced amplification of water velocity could result in substantial spatial variation in wave-induced hydrodynamic forces and might thereby help to explain the patchwork nature of disturbance that is characteristic of intertidal communities.

Physical disturbance caused by wave-induced forces is an important determinant of ecological structure and community dynamics in the intertidal zone of wave-swept rocky shores (e.g., Dayton 1971; Paine and Levin 1981; Denny and Wethey 2000). As a means of quantifying spatial and temporal patterns in surf zone water velocities, several studies have used recording dynamometers to measure the maximum hydrodynamic forces imposed on small objects in the intertidal zone (e.g., Jones and Demetropoulos 1968; Denny et al. 1985; Bell and Denny 1994; Vogel 1994; Gaylord 1999; Denny and Wethey 2000). If it is assumed that the force imposed on each object (usually a sphere) is attributable solely to drag (*see* Gaylord 2000), these measurements can then be used to estimate U_{max}, the maximal wave-induced water velocity that occurs in the surf zone (Eq. 1).

$$U_{max} = \sqrt{\frac{2F}{\rho A C_d}} \quad (1)$$

Here, F is the imposed force, ρ is the density of seawater (1,025 kg m^{-3}), A is the projected area of the object, and C_d is a dimensionless drag coefficient (which might vary slightly with velocity, *see* Bell and Denny 1994). The forces reported to date suggest that water velocities of 16–20 m s^{-1} can be present when ocean waves break on rocky shores (Jones and Demetropoulos 1968; Denny et al. 1985; Bell and Denny 1994; Vogel 1994; Denny 1995), and measurements reported here extend this range to 25 m s^{-1}.

These extreme velocities and the forces attributable to them—each a major component of ''wave exposure''—can have substantial biological significance: They can limit the local range of species (e.g., Denny 1995; Shaughnessy et al. 1996; Graham 1997), they can limit the size of individuals (e.g., Carrington 1990; Dudgeon and Johnson 1992), and they can cause disturbance that affects community dynamics (e.g., Dayton 1971; Menge 1976; Sousa 1979; Paine and Levin 1981).

An attempt has been made at a mechanistic prediction of these effects (Denny 1995). In this approach, the statistics of the random sea are used to predict the maximum height of waves as they break on the shore, and wave theory is then used to predict the maximum water velocity associated with a wave of that height. The hydrodynamic forces imposed by that water velocity (drag, lift, or the ''impingement force,'' Gaylord 2000) can then be predicted as a function of the size and shape of the organism on which the velocity is imposed. A comparison of that maximal force with the strength of the organism allows for a prediction of whether the organism will be broken or dislodged, thereby providing quantitative information regarding the effect of wave climate on community ecology.

As straightforward as this approach appears to be in the-

[1] Corresponding author (mwdenny@leland.stanford.edu).
[2] Present address: Marine Physical Laboratory, Scripps Institution of Oceanography, La Jolla, California 92037.
[3] Present address: Department of Biological Sciences, University of South Carolina, Columbia, South Carolina 29208.

Acknowledgments

This research was supported by NSF grant OCE 9985946 to M.W.D. We thank two anonymous reviewers for helpful comments.

ory, there has been at least one major complication to its employment in practice: Velocities measured near the substratum using dynamometers often exceed those of oncoming waves. The maximum velocity that occurs in a breaking wave is equal to the speed of the waveform, the phase speed. According to solitary wave theory, phase speed of a breaking wave is approximately equal to Eq. 2.

$$U_{\max} = \sqrt{g(d + H)} \tag{2}$$

g is the acceleration due to gravity (9.8 m s^{-1}), d is the still-water depth of the water column under the breaking wave, and H is the wave height (*see* Munk 1949; Carstens 1968; Denny 1988). For the steep beach slopes characteristic of many rocky shores, $d \approx H$ when waves break (Galvin 1972), giving Eq. 3.

$$U_{\max} \approx \sqrt{2gH}, \quad \text{and} \quad H \approx \frac{U_{\max}^2}{2g} \tag{3}$$

Thus, if the maximum wave-induced velocity imposed on the shore is 25 m s^{-1}, the predicted breaking height must be nearly 32 m. This height rivals that of the highest ocean wave ever measured (33.5 m, Whitemarsh 1934) and is more than twice that of the highest waves predicted to occur in a typical year in the coastal waters of the west coast of the United States (~13 m, Denny 1995).

How can we reconcile the relatively slow velocities predicted for breaking waves with the apparent extreme velocities encountered in the intertidal zone? One possibility is that the interaction of wave-induced flows with the three-dimensional topography of the rocky shore somehow amplifies the water velocity. Although this possibility has been suggested previously (e.g., Peregrine 1995), theoretical and experimental research in the interaction of breaking waves with shoreline structures has been confined primarily to two-dimensional shores—that is, to structures (such as breakwaters) in which the topography varies in the onshore–offshore direction but is everywhere the same along the shore (e.g., Kobayashi and Demirbilek 1995; Kobayashi 1999; Bullock et al. 2001). A few studies have examined wave-induced flows around vertical cylinders (reviewed in Kobayashi 1999). Cylinders and two-dimensional breakwaters cannot represent the topographical complexity that is characteristic of rocky shores. Furthermore, engineering studies have focused on predicting the pressure applied to shoreline structures; therefore, they speak primarily to the forces directed normal to the substratum. These forces are likely to have little effect on benthic organisms. For example, an acorn barnacle has a strong, rigid test filled with virtually incompressible materials (water and the barnacle's body). Any sudden increase in external pressure on the barnacle's test is resisted by the constant volume of body within; therefore, damage is unlikely. In contrast, flow parallel to the substratum can impose drag and lift forces that push the organism sideways or pull it away from the substratum, and these forces are potentially dangerous (*see* Denny 1988, 1995; Denny and Wethey 2000). Information regarding flow relevant to intertidal organisms (flow parallel to the substratum) is difficult to extract from the engineering studies conducted to date, and Kobayashi (1999) notes that even numerical modeling of the flow around three-dimensional structures of arbitrary shape will be challenging.

Here, we report empirical measurements of wave-driven flows associated with a three-dimensional beach—a small-scale promontory of the sort commonly found on rocky shores. We show that when a broken wave (a turbulent bore) is refracted by the promontory, the leading edge of the waveform is bent into two limbs that collide. The resulting interaction can produce a localized jet with a velocity nearly twice the phase speed of the incident bore. The flow speed in this jet can be further amplified by a factor of 1.3–1.6 if the horizontal jet encounters a vertical wall. These topographical effects could easily amplify the phase speed of even relatively small waves to the extreme values that have been recorded in the intertidal zone.

Materials and methods

Recording dynamometers of the design described by Denny and Wethey (2000) were deployed at 221 sites on the shore adjacent to Hopkins Marine Station (HMS) in Pacific Grove, California. Each dynamometer recorded the maximum hydrodynamic force imposed on a small, perforated plastic sphere (a wiffle golf ball, 40.8 mm diameter) during the 2–7 d of a deployment. In the period from October 1997 to May 1999, an average of 38 deployments were conducted per site. Dynamometers were calibrated in the laboratory as detailed by Bell and Denny (1994). The maximum forces recorded by each dynamometer, F (newtons, N), were converted to equivalent velocities (m s^{-1}) using a modification of Eq. 1, as suggested by Bell and Denny (1994).

$$U_{\max} = {}^{1.93}\sqrt{\frac{F}{0.575}} \tag{4}$$

We desired to measure the height of waves that could have caused the extreme velocities recorded at HMS. To this end, we installed a bottom-mounted wave gauge (SeaBird SBE 26-03 Seagauge) at a depth of 10 m ~50 m offshore of the sites where force measurements were conducted. Significant wave height (H_s, the average height of the highest one third of all waves) and peak wave period (T) were recorded every 6 h from October 1997 through December 2001. Longuet-Higgins (1952, 1980) provides a means of calculating, from the significant wave height, the maximal height of an individual wave that can be expected in time t (in this case, 6 h; Eq. 5).

$$H_{\max} = 0.654H_s\{[\ln(t/T)]^{1/2} + 0.289[\ln(t/T)]^{-1/2}\} \tag{5}$$

See Denny (1988, 1995) for a more complete explanation of the statistics of maximal wave heights.

The effect of shoreline topography on water velocity was explored in a laboratory wave tank (Fig. 1). The tank is 8.2 m long and 1.8 m wide, with walls 1.1 m high. The depth of the water column (in the absence of waves) was 61 cm. Single waves were produced at the proximal end of the tank and propagated to the distal end, where they interacted with one of a series of ''beaches'' (Fig. 1). After this interaction, flow in the tank was allowed to subside before the wave-making apparatus was reset and the experiment was repeat-

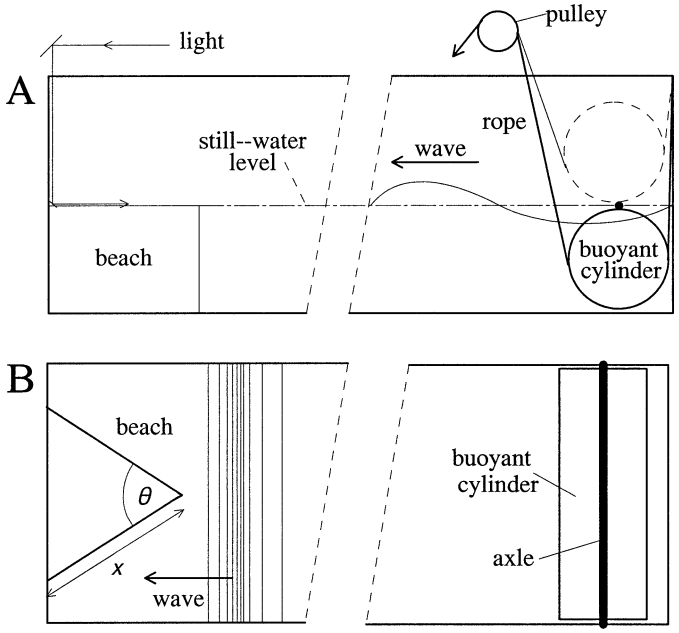

Fig. 1. A schematic drawing of the wave tank used in these experiments (not to scale). (A) Side view. A sheet of light from a slide projector reflects off two mirrors and travels parallel to the horizontal surface of the beach. A single wave is produced by the motion of a buoyant cylinder, which rotates around a horizontal axle anchored to the sides of the tank. When, under the urging of a rope, the cylinder ''flips up,'' water moves into the space vacated by the cylinder. This inflowing wave is reflected from the end of the tank and subsequently travels toward the beach as shown. After water motion in the tank has ceased, the apparatus is reset by sinking the cylinder and then filling it with air. (B) Top view showing the beach angle, θ, and the length of the beach walls, x.

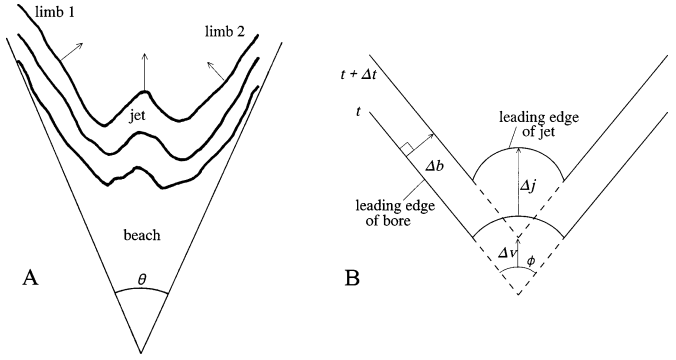

Fig. 2. (A) A typical tracing of the leading edge of a refracted bore (with two limbs) as it traverses the beach (view from above). The outline of the beach is shown for reference. In this case, the beach angle $\theta = 45°$. (B) The refracted bore and the resulting jet are shown schematically at two times as they traverse the horizontal surface of the beach. The angle, ϕ, between the refracted limbs of the bore could be different from the beach angle, θ. In time Δt, each limb travels a distance Δb, so its phase speed is $\Delta b/\Delta t$. In the same period, the jet travels a distance Δj, so its speed is $\Delta j/\Delta t$. The theoretical intersection between limbs (in the absence of a jet) would occur at the location shown by the dashed lines. The speed of this intersection is $\Delta v/\Delta t$.

ed. Each beach formed a prow extending from the distal wall of the tank. This combination of a ''step'' backed by a vertical wall is a rough model of topography commonly found on rocky shores. The vertical walls of the hollow, box-like beach were constructed from braced plywood and were 61 cm high (equal to still-water depth). The length of these walls (x in Fig. 1B) was 1.1 m, and the top of the prow (a sheet of plywood) was horizontal. The angle presented to the wave (θ, *see Fig. 1*) varied from 45 to 105° in 15° increments. No effort was made to seal the edges of the beach, and some water inevitably moved between the beach's exterior and interior during wave breaking. Note that because of the fixed length of the beach walls, varying lengths of the distal wall of the tank were exposed to the incident waves depending on the beach angle.

As each wave encountered the beach, it was refracted by the beach's sides, forming two limbs of a turbulent bore that propagated across the horizontal surface of the beach (Fig. 2A). The interaction between these limbs was recorded by a video camera mounted approximately 4 m vertically above the beach surface. To assist in the visualization of these interactions, light was transmitted via two mirrors such that a thin (~5 mm), horizontal sheet of light was projected parallel and adjacent to the beach surface toward the oncoming limbs of the bore. The light sheet was produced by a slide projector that projected a horizontal slit. The room lights were turned off during each experiment, with the result that the leading edge of the refracted bore near the substratum was recorded as a bright line as the limbs traversed the beach through the light sheet (Fig. 2A). Subsequent calibration of the image size with a ruler placed on the beach allowed the velocity of the leading edges of the limbs to be calculated from a frame-by-frame analysis of the video recordings. Images of each experiment were recorded at 30 frames s^{-1} (60 fields s^{-1}) using a Pulnix TMC-514 camera, and each field was time-stamped using a Horita TG-50 time code generator and recorded on a Sony EVS5000 Hi8 video cassette recorder. At least 10 replicate experiments were conducted for each beach angle.

Windows in the side of the wave tank allowed for a video measurement of the height of waves as they approached the beach. These measurements required the room lights to be on; therefore, wave height measurement could not be conducted simultaneously with the measurements of bores traversing the beach.

For each video frame of each experiment measurements were made (*see Fig. 2B*) of (1) the location of the leading edge of each of the two limbs of the refracted bore, (2) the angle, ϕ, between the limbs of the bore, and (3) the leading edge of the jet formed at the intersection of the limbs. From these data, we calculated (1) the speed of the limbs ($\Delta b/\Delta t$ in Fig. 2B) averaged through the experiment, (2) the average angle between the limbs, and (3) the speed of the jet ($\Delta j/\Delta t$ in Fig. 2B), again averaged through the experiment. Typically six to eight consecutive frames were used to characterize each experiment. Average speeds were calculated for each limb of the bore by measuring $\Delta b/\Delta t$ along each of three lines lying parallel to the direction of the limb's propagation. Similarly, the average speed of the jet was calculated from values of $\Delta j/\Delta t$ measured along each of three

lines within the jet, each line lying parallel to the direction of the jet's motion.

After refracted bores and their associated jets had traversed the beach, they impacted on the vertical distal wall of the tank. The speed of the resulting upward flow (the ''splash'') was measured in a separate set of experiments. The lower mirror (Fig. 1) was removed from the beach, and the upper mirror was adjusted so that a sheet of light was projected downward parallel to the distal wall and extending approximately 5 mm out from it. With the room lights extinguished, the leading edge of the flow up the distal wall appeared as a bright line. These experiments were recorded at 60 frames s^{-1} using a Redlake MotionScope PCI 1000S digital high-speed video camera. The camera viewed the scene through the side windows of the tank, and the images were calibrated by placing a ruler on the distal wall. Ten replicates were conducted for each beach angle, with the exception of the 60° beach, for which 20 replicates were conducted. Images of the jet and bore silhouetted against the illuminated back wall of the tank allowed for an estimation of the height of the jet and bore as they approached the wall.

As with the experiments regarding the interactions of the limbs of the bore, the speed of the splash up the distal wall was measured from a frame-by-frame analysis. The average speed of flow was calculated as the least-squares linear regression of the location of the leading edge of the splash as a function of time. Typically 6–11 frames were used in each regression. Although one might expect the speed of the flow in the splash to decrease with time as water is accelerated downward by gravity, we found that actual speeds were surprisingly constant through the duration of our measurements; therefore, a linear regression provided an appropriate measure of the average speed; $r^2 > 0.99$ were typical. Note that our experiment was designed specifically to measure the flow adjacent to the distal wall. Much of the splash occurred away from the wall, and this bolus of water tended to obscure the view of near-wall flow during the later portions of each event. As a result, our estimates of speed are taken from the initial portions of the experiments, during which the flow was still strongly affected by the impact of the jet and bore and the ballistic deceleration due to gravity was likely to be least evident.

The results of these experiments can be presented either in absolute or relative terms: the speed of bores, jets, and splash or the ratios of jet-to-bore speeds, splash-to-bore speeds, or splash-to-jet speeds. Because the speeds of jets and bores were measured simultaneously, there is no problem in calculating their ratio. However, because splash speeds could not be measured in the same experiments, the ratios of splash-to-bore and splash-to-jet speeds can only be calculated as averages. The range of averages and the variability of splash-to-bore and splash-to-jet ratios are estimated by the following procedure. The bore speeds for the replicated experiments at one beach angle were ranked in ascending order, paired with the separately measured splash speeds, likewise ranked in ascending order. For each pair, the ratio of splash to bore speed was calculated and the average and standard deviations of these ratios were determined. This procedure (which, in effect, assumes that the lowest splash velocity was caused by the lowest bore velocity recorded in the separate experiments and the highest splash velocity by the highest bore velocity) provides one estimate of the mean ratio of speeds and an estimate of the minimum variation among splash-to-bore speed ratios. Alternatively, bore speeds were ranked in ascending order and paired with splash speeds ranked in *descending* order. The ratio of splash-to-bore speed was calculated for each pair, and the average and standard deviations of these ratios were determined. This procedure (which assumes, probably unrealistically, that the lowest splash velocity was caused by the highest bore velocity) provides a separate estimate of the average ratio and an estimate of the maximum variation among splash-to-bore speed ratios. In all probability, the actual ratio of splash-to-bore speed lies between these two estimates. The same procedure was used to calculate the ratio of splash-to-jet speeds.

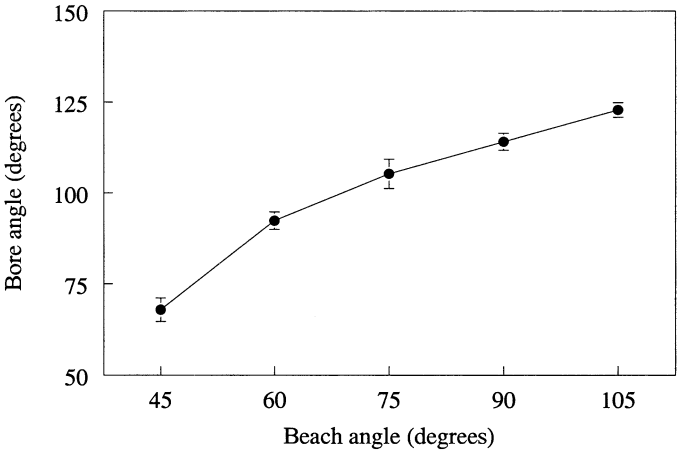

Fig. 3. The mean bore angle, ϕ (solid circles ± SEM), is greater than the beach angle, θ.

Results

Field—The maximum force recorded by dynamometers deployed in the field was 303 N, corresponding to an equivalent velocity of 25.7 m s^{-1} (Eq. 4). The site at which this measurement was made lies on a vertical wall situated shoreward of a horizontal bench similar to the ''step'' in our model experiments. The vertical wall faces directly into the oncoming waves. In 21 instances (at four different sites, each on a vertical wall), equivalent velocities in excess of 20 m s^{-1} were recorded.

The highest significant wave height recorded in the 50 months of our experiment was 3.37 m with a period of 9 s. If we assume that this sea state was present for the entire 6 h until the next measurement was made, the height of the expected individual highest wave incident on the shore at HMS was 5.66 m (Eq. 5). We assume that this is approximately equal to the height of the wave at breaking and use this value to estimate the maximal phase speed of bores in the surf zone.

Laboratory—The height of the waves impinging on the laboratory beach was 17.1 cm with a standard deviation of

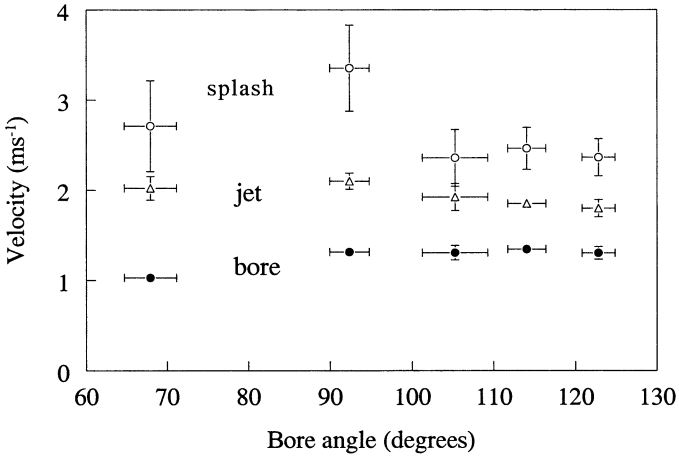

Fig. 4. The speeds of bores, jets, and splash as a function of bore angle. The speeds of both jets and splash are substantially higher than the phase speed of the bores. Open circles, splash velocities; triangles, jet velocities; filled circles, bore velocities. Error bars are standard deviations.

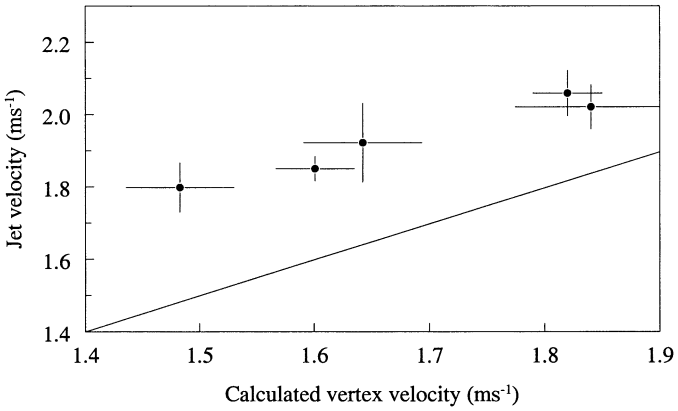

Fig. 5. The measured velocities of the jet lie above the line depicting the calculated velocity of the vertex between interacting limbs of the bore. All error bars are 95% confidence limits. The scatter in the data with respect to calculated vertex velocity is due to variation both in the phase speed of bores and in the bore angle.

0.4 cm. The waves resembled spilling breakers in that they had a turbulent leading face near the wave crest. The refracted limbs of the bores near the distal wall had an average height of 6.4 cm (SD = 1.2 cm), with no apparent pattern of variation across beach angles.

The angle between the limbs of the bore, ϕ, increased with the beach angle, θ (Fig. 3), and there was little variation in angle among replicates.

For each bore angle, ϕ, jet velocity exceeded the bore velocity, and splash velocity exceeded that of both the jet and the bore (Fig. 4). It is perhaps not surprising that the jet velocity exceeds the bore velocity. If the leading edge of flow were to be recorded at the geometrical vertex between the two limbs of the refracted bore, Eq. 6 would describe the apparent velocity measured ($\Delta v/\Delta t$ in Fig. 2B).

$$\text{vertex velocity} = \frac{\text{bore velocity}}{\sin(\phi/2)} \qquad (6)$$

Because ϕ in these experiments is always less than 180°, $\sin(\phi/2) < 1$, and the vertex velocity must exceed the bore velocity. Furthermore, in these experiments, a distinct jet of water is typically formed at the vertex between the limbs of the refracted bore and is projected forward, ahead of the geometric vertex. As a result, the jet velocities recorded here are significantly in excess of the vertex velocity calculated by Eq. 6 (*see Fig. 5*).

The ratio of jet speed to bore speed decreases with increasing bore angle, varying from nearly 2.0 at a bore angle of 68° (a beach angle of 45°) to ~1.4 at bore angles of 114–122° (beach angles of 90 and 105°, respectively, Fig. 6A).

The ratio of splash velocity to bore velocity also decreases with increasing bore angle from approximately 2.6 at a bore angle of 68° to approximately 1.8 at bore angles of 114 and 122° (Fig. 6A).

The ratio of splash velocity to jet velocity shows no clear pattern with bore angle (Fig. 6B). When the bore angle is 92° (beach angle, 60°), splash velocity is approximately 1.6 times jet velocity, but at all other bore angles, splash velocity is approximately 1.3 times that of the jet. The unusually high splash velocities measured at a bore angle of 92° were verified with a second set of 10 replicates. The mechanistic reason for the high splash speeds at this bore angle is not

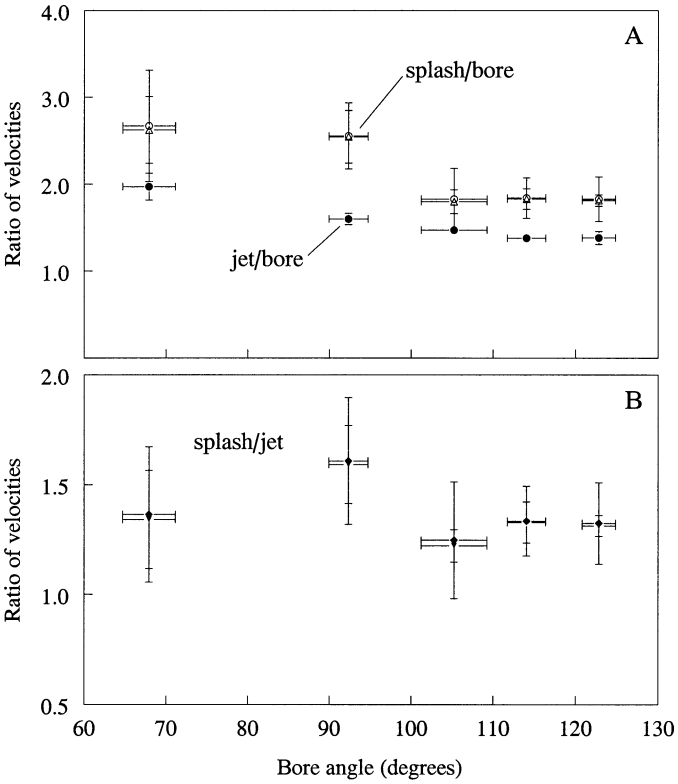

Fig. 6. Ratios of velocities as a function of bore angle, ϕ. (A) Jet-to-bore velocities (open circles and triangles) and splash-to-bore velocities (filled circles). (B) Splash-to-jet velocities. Error bars are standard deviations. The two data sets for the splash-to-bore and splash-to-jet ratios are due to the two manners in which these ratios were calculated (*see text*).

immediately apparent. The confluence of the jet and the limbs of the bore at the wall simply appears to be ''right'' to result in an atypically high splash velocity.

These experiments demonstrate that at least two mechanisms are available whereby the topography of a rocky shoreline could amplify the speed of flow in broken waves. The interaction of bores arriving from different directions (in this case, by refraction at a promontory) can form a jet in which the flow can approach speeds twice the phase speed of the bore. Speeds can also be augmented when bore-driven flows across horizontal surfaces arrive at a vertical wall. In this case, speed at the wall is typically enhanced by a factor of 1.3 but might be enhanced by as much as a factor of 1.6.

Discussion

The speed amplifications measured in these experiments are sufficient to account for the extreme apparent velocities measured on wave-swept shores. For example, a wave 5.66 m high at breaking (the maximum height estimated from wave records for the site at which 25 m s^{-1} velocities have been recorded) should be accompanied by velocities of approximately 10.5 m s^{-1} (Eq. 3). If this wave is refracted by the shore such that the resulting limbs interact with each other at an angle of 68°, the resulting splash velocity on a vertical rock face could be amplified by a factor of 2.6 (Fig. 6A): 10.5 m $s^{-1} \times 2.6 = 27.3$ m s^{-1}. Even on a horizontal beach, the velocity associated with the jet created by this interaction would be 21 m s^{-1}, twice the bore velocity (Fig. 6A).

These results suggest that when predicting the biological effects of wave-induced flows, it will not be sufficient simply to calculate the phase speed of waves impinging on the shore. Instead, at least a second step must be included in which the effects of small-scale shoreline topography are taken into account. For example, an organism living on a vertical face might commonly experience flow speeds 1.3–1.6 times those of nearby organisms living on horizontal surfaces. Because drag and lift vary with the square of water velocity, the organism on the vertical face would experience forces $1.3^2 - 1.6^2 = 1.7$–2.6 times those of its neighbors. This local difference in imposed force could contribute to differences in the communities present. For instance, Blanchette (1994) noted that the mussel *Mytilis californianus* outcompeted the sea palm *Postelsia palmaeformis* on horizontal rock surfaces but that the order of dominance was reversed on adjacent vertical surfaces. Schoch and Dethier (1996) noted that much of the variation in organismal abundance at a site in the San Juan Islands (Washington state) was associated with differences in the slope of the shore. Similarly, stretches of shoreline on which bores are refracted and interact might typically experience faster flows and larger forces than nearby stretches on which bores do not commonly interact. This topographically influenced local variation in force might go far toward explaining the patchwork nature of disturbance that is characteristic of intertidal communities (e.g., Paine and Levin 1981).

The specific fluid dynamic mechanisms responsible for the formation of the jet and the augmented velocity of the splash remain to be elucidated. An observation and a speculation might aid in this exploration. First, if the two limbs of the refracted bore interacted as separate waveforms, one would expect that as they collide they would superimpose and move through each other. If this happened, the point of intersection between the limbs should have a height substantially higher than that of either limb itself, and the portions of the limbs that lie ''seaward'' of the intersection should be evident in the lee of each limb. Neither is the case for the bores in our experiments. There is no evidence visible in the video data that either the intersection between limbs or the jet itself has a wave height greater than the bore's limbs. Thus, the increased velocity of the jet cannot be attributed to increased wave height. The limbs of the bore do not pass through each other; therefore, they do not appear to act as separate waveforms. Instead, the limbs appear to act as two separate masses of water moving ballistically across the beach. Where they collide, water is ''squeezed'' horizontally forward, forming the jet. In this respect, the jet formed in our experiment is a two-dimensional analog to the jet of molten metal that is formed during the detonation of the shaped charge in a bazooka shell (*see* p. 395–396 in Batchelor 1967). Unfortunately, the analogy is only qualitative. The speed of jet formed by our colliding limbs is much lower than that predicted by the theory of shaped charges. Finally, we speculate that the amplification of velocity in the splash is due primarily to the principle of continuity (*see* Vogel 1994). As the jet and the limbs of the bore converge, a substantial volume of moving water arrives at a small area of the vertical distal wall. Constrained from moving away from the wall by the inertia of the inflow, the only path along which water can escape is through a relatively small area up the wall. In essence, the convergence of the jet and limbs might act in the same fashion as the thumb one places over the end of a hose to speed up the outflow.

Two caveats should be noted in regard to the conclusions reached here. First, we do not mean to imply that the mechanisms described above are the only ones capable of amplifying velocities in the surf zone. Many other mechanisms could exist. For example, as flow moves past the corner of an object (for instance, as a wave passes a sharp-edged boulder), an irrotational vortex can be formed in the object's wake (Batchelor 1967). Velocity in such a vortex varies roughly as $U_{max} r_{max}/r$, where U_{max} is again the phase speed of the wave, r_{max} is the overall radius of the vortex, and r is distance from the center of the vortex (Batchelor 1967; Vogel 1994). Clearly this relationship cannot hold very near the vortex's center (there will be a rotational vortex at the core, *see* Vogel 1994), but it is not unreasonable to expect that velocities considerably in excess of U_{max} could exist and can be imposed on the substratum if the vortex is shed downstream. Flows can also be enhanced in surge channels when propagating bores are squeezed laterally by the walls of the channel in an effect again similar to placing one's thumb over the end of a hose. Amplification of velocities on vertical walls can occur even on two-dimensional shores as water is caught between an advancing wave and the wall. The resulting squeeze results in a ''flip through'' of the water's surface and rapid upward acceleration of the water (*see* the review by Peregrine 1995).

Second, we note that the extreme velocities cited above (16–25 m s^{-1}) were calculated on the assumption that drag was the sole force imposed on the recording dynamometers (*see Eq. 1*). The drag coefficient used in these calculations was measured in steady flow while the drag element was always submerged (Bell and Denny 1994). Gaylord (2000) has shown, however, that when a wave strikes an intertidal object, the force associated with the initial immersion of the object (the ''impingement'' force) can be two to three times that predicted for drag alone. In this case,

$$U_{\max} = \sqrt{\frac{2F}{\rho A C_i}} \tag{7}$$

C_i (the impingement coefficient) can be two to three times C_d. Thus, if the maximum force recorded by wave-swept transducers is caused by impingement, the predicted maximum velocity in the breaking wave could be smaller than that we have cited here by a factor of $\sqrt{2}$ to $\sqrt{3}$. That is, the maximum velocities imposed on wave-swept shores might be only 14–16 m s^{-1} rather than 25 m s^{-1}.

If this were true, it would raise a question as to whether the velocity amplification mechanisms proposed here actually operate in nature. If they do, the extreme velocities they should cause (as high as 27 m s^{-1}, calculated above), are substantially higher than the maximum velocities calculated from the impingement force (14–16 m s^{-1}). However, the forces used to calculate maximal water velocity were recorded using spring-based dynamometers. Although the response time of these dynamometers is difficult to measure directly (*see* Bell and Denny 1994), the compliance of the device ensures that briefly applied forces will be under-recorded. Impingement forces, although large, are exceedingly brief. They typically peak in less than 0.05 s (Gaylord 1999), far too short to be recorded accurately by the dynamometers. In other words, although impingement forces are likely to play an important role in surf zone mechanics (Gaylord 2000), their effects are unlikely to have substantially contaminated the force measurements used here as a basis for calculating maximum velocity.

Similar logic leads us to suppose that forces imposed on the dynamometers by the water's acceleration are negligible. Denny et al. (1985) and Gaylord et al. (1994) proposed that the extreme accelerations present in turbulent surf zone flows could impose large forces on wave-swept objects. Although the accelerations present in surf zone flows can indeed be impressive (often in excess of 100 m s^{-2}, Denny et al. 1985; Gaylord 1999), Gaylord (2000) has shown that the spatial scale of these accelerations is far too small for the acceleration of the water to impose an appreciable force on objects the size of the wiffle balls used in our experiments. Therefore, we continue to suspect that velocities in the range of 20–25 m s^{-1} indeed occur in the surf zone of wave-swept shores, leaving plenty of room for flow amplification mechanisms to be effective.

The wave-induced water velocities reported here have been characterized by a comparison to the measured phase speed of a bore as it traverses the beach. In contrast, speeds measured in the field have been compared to the calculated phase speed of incident waves as they break on the beach. Why have we chosen bore speed rather than incident wave speed as the standard for our experiments? On a real shore, the two speeds should be nearly the same. Until the breaking wave loses substantial energy to turbulent processes or run-up, the phase speed of the broken wave will be approximately equal to the phase speed of the incident wave as it breaks (Carstens 1968; Galvin 1972; U.S. Army Corps of Engineers 1984). In our experiments, however, the two speeds are substantially different. The incident wave (with a height of 17 cm and a still-water depth of 61 cm) has a phase velocity of nearly 2.8 m s^{-1} (Eq. 2), whereas the bores (with a height of approximately 6.4 cm) traverse the beach with a measured velocity between 1.0 and 1.3 m s^{-1}. This drastic reduction in bore height (and, therefore, phase speed) is likely due at least in part to the manner in which waves break on our hollow beach. Because some water can move into the beach during initial contact with the incident wave, there is less of an impetus for water to be forced onto the beach as a bore and the resulting bore height is lower than it would be on a real shore. It is because of this artifact that we have chosen to use bore speed rather than incident-wave phase speed as our standard.

Our experiments show that the interaction between bores can produce jets in which the velocity is nearly twice the bores' phase speed. This velocity can be further amplified by a factor of 1.3–1.6 if the jet strikes a vertical wall and, together the two mechanisms of amplification, can account for the extremely high velocities recorded in the surf zone of rocky shores. These types of topographically induced amplification of water velocity could result in substantial spatial variation in wave-induced hydrodynamic forces and might thereby help to explain the patchwork nature of disturbance that is characteristic of intertidal communities.

References

BATCHELOR, G. K. 1967. An introduction to fluid mechanics. Cambridge Univ. Press.

BELL, E. C., AND M. W. DENNY. 1994. Quantifying ''wave exposure'': A simple device for recording maximum velocity and results of its use at several field sites. J. Exp. Mar. Biol. Ecol. **181:** 9–29.

BLANCHETTE, C. A. 1994. The effects of biomechanical and ecological factors on population and community structure of wave-exposed intertidal macroalgae. Ph.D. thesis, Oregon State Univ.

BULLOCK, G. N., A. R. CRAWFORD, P. J. HEWSON, M. J. A. WALKDEN, AND P. A. D. BIRD. 2001. The influence of air and scale on wave impact pressures. Coast. Eng. **42:** 291–312.

CARRINGTON, E. 1990. Drag and dislodgment of intertidal macroalgae: Consequences of morphological variation in *Mastocarpus papillatus* Kützing. J. Exp. Mar. Biol. Ecol. **139:** 185–200.

CARSTENS, T. 1968. Wave forces on boundaries and submerged bodies. Sarsia **34:** 37–60.

DAYTON, P. 1971. Competition, disturbance, and community organization: The provision and subsequent utilization of space in a rocky intertidal community. Ecol. Monogr. **41:** 351–389.

DENNY, M. W. 1988. Biology and the mechanics of the wave-swept environment. Princeton Univ. Press.

———. 1995. Predicting physical disturbance: Mechanistic approaches to the study of survivorship on wave-swept shores. Ecol. Monogr. **65:** 371–418

———, AND D. WETHEY. 2000. Physical processes that generate

patterns in marine communities, p. 3–37. *In* M. D. Bertness, S. D. Gaines, and M. E. Hay [eds.], Marine community ecology. Sinauer.

———, T. L. DANIEL, AND M. A. R. KOEHL. 1985. Mechanical limits to size in wave-swept organisms. Ecol. Monogr. **55:** 69–102.

DUDGEON, S. R., AND A. S. JOHNSON. 1992. Thick vs. thin: Thallus morphology and tissue mechanics influence differential drag and dislodgment of two co-dominat seaweeds. J. Exp. Mar. Biol. Ecol. **165:** 23–43.

GALVIN, C. J. 1972. Wave breaking in shallow water, p. 413–455. *In* R. E. Meyer [ed.], Waves on beaches and the resulting sediment transport. Academic.

GAYLORD, B. 1999. Detailing agents of physical disturbance: Wave-induced velocities and acceleration on a rocky shore. J. Exp. Mar. Biol. Ecol. **239:** 85–124.

———. 2000. Biological implications of surf-zone complexity. Limnol. Oceanogr. **45:** 174–188.

———, C. A. BLANCHETTE, AND M. W. DENNY. 1994. Mechanical consequences of size in wave-swept algae. Ecol. Monogr. **64:** 287–313.

GRAHAM, M. H. 1997. Factors determining the upper limit of giant kelp, *Macrocystis pyrifera* Aaagardh, along the Monterey peninsula, central California, USA. J. Exp. Mar. Biol. Ecol. **218:** 127–149.

JONES, W. E., AND A. DEMETROPOULOS. 1968. Exposure to wave action: Measurements of an important ecological parameter on rocky shores of Anglesey. J. Exp. Mar. Biol. Ecol. **2:** 46–63.

KOBAYASHI, N. 1999. Numerical modeling of wave runup on coastal structures and beaches. Mar. Tech. Soc. J. **33:** 33–37.

———, AND Z. DEMIRBILEK [EDS.]. 1995. Wave forces on inclined and vertical structures. American Society of Civil Engineers.

LONGUET-HIGGINS, M. S. 1952. On the statistical distribution of the heights of sea waves. J. Mar. Res. **11:** 245–266.

———. 1980. On the distribution of the heights of sea waves: Some effects of nonlinearity and finite band width. J. Geophys. Res. **85**(C3): 1519–1523.

MENGE, B. 1976. Organization of the New England rocky intertidal community: Role of predation, competition, and environmental heterogeneity. Ecol. Monogr. **46:** 355–393.

MUNK, W. H. 1949. The solitary wave theory and its application to surf problems. Ann. N.Y. Acad. Sci. **51:** 376–424.

PAINE, R. T., AND S. A. LEVIN. 1981. Intertidal landscapes and the dynamics of pattern. Ecol. Monogr. **51:** 145–178.

PEREGRINE, D. H. 1995. Water wave impact on walls and the associated hydrodynamic pressure field, p. 259–281. *In* N. Kobayashi and Z. Demirbilek [eds.], Wave forces on inclined and vertical structures. American Society of Civil Engineers.

SCHOCH, G. C., AND M. N. DETHIER. 1996. Scaling up: The statistical linkages between organismal abundance and geomorphology on rocky intertidal shorelines. J. Exp. Mar. Biol. Ecol. **201:**37–72.

SHAUGHNESSY, F. J., R. E. DEWREEDE, AND E. C. BELL. 1996. Consequences of morphology and tissue strength to blade survivorship of two closely related rhodophyta species. Mar. Ecol. Progr. Ser. **136:** 257–266.

SOUSA, W. 1979. Disturbance in marine intertidal boulder fields: The nonequilibrium maintenance of species diversity. Ecology **60:** 1225–1239.

U.S. ARMY CORPS OF ENGINEERS. 1984. Shore protection manual, 4th ed.). U.S. Government Printing Office.

VOGEL, S. 1994. Life in moving fluids, 2nd ed. Princeton Univ. Press.

WHITEMARSH, R. P. 1934. Great sea waves. U.S. Naval Inst. Proc. **60:** 1094–1103.

Received: 4 March 2002
Accepted: 30 August 2002
Amended: 11 September 2002